

SCIENTIA
IRANICA

Sharif University of Technology

Scientia Iranica

Transactions C: Chemistry and Chemical Engineering

www.scientiairanica.com



Enhancement of hydrogen storage on multi-walled carbon nanotube through KOH activation and nickel nanoparticle deposition

A. Hosseini, A.A. Ghoreyshi*, K. Pirzadeh and M. Mohammadi

Department of Chemical Engineering, Babol University of Technology, Babol, Iran.

Received 2 August 2015; received in revised form 28 October 2016; accepted 20 February 2017

KEYWORDS

Multi-walled carbon nanotube;
Chemical activation;
Hydrogen adsorption;
Electroless metal deposition;
Hydrogen storage.

Abstract. Hydrogen uptake of multi-walled carbon nanotube (MWCNT) was enhanced via a two-step activation/deposition process. At the first step, MWCNT was chemically activated by KOH. The hydrogen uptake of the activated MWCNT was considerably higher than the pristine one. The BET analysis of the activated MWCNT demonstrated a great improvement in its textural properties compared to the pristine MWCNT. This was attributed to the defects generated on its external surface during activation process as evidenced by Raman and SEM analyses. At the second step, electroless deposition technique without any surface pretreatment was employed for preparation of Ni-MWCNT composite. The successful deposition of nickel into the activated MWCNT was approved by the EDS analysis and its amount was determined by ICP spectroscopy which was 2.8 wt.% with respect to Ni available in the electroless deposition bath. The maximum H₂ storage capacity achieved by Ni doped MWCNT sample was ~ 1 wt.% at 288 K and 45 bar.

© 2017 Sharif University of Technology. All rights reserved.

1. Introduction

Nowadays, there is a tremendous demand for clean, inexpensive and sustainable energy sources due to public concerns and environmental hazards raised by overusing fossil fuels. Therefore, lots of attempts have been made to exploit alternative sources of energy. Among renewable energies, hydrogen is considered as a very promising source of energy owing to its high-energy density, plentiful supply, and pollution-free combustion [1,2]. These characteristics make hydrogen as an attractive energy carrier. However, a major problem that researchers have encountered in the development of fuel cells technology is the safe storage of hydrogen in an affordable system [3].

There are several factors that affect the selection of a suitable technique for hydrogen storage includ-

ing high storage capacity, suitable thermodynamic properties, fast adsorption/desorption kinetics, high safety and process economy. In recent years, many investigations have been carried out to develop materials and methods for safe and inexpensive storage of hydrogen. Currently, there are three hydrogen storage methods: compression at high pressure, liquefaction at low temperature, and chemical and/or physical adsorption on solid porous media. Hydrogen storage by compression at high pressure is not safe due to the risk of explosion. The second technique suffers from large energy requirement to maintain the low temperature. Solid porous materials are considered as a promising and effective route for storing hydrogen [4].

The target posed by the DOE is hard to reach and cannot be achieved by any existing system. At present, metal hydrides outperform all investigated materials as hydrogen storing media due to their high storage capacity [5]. However, heavy weight, high production costs, high temperature needed for

*. Corresponding author. Tel.: +98-(111)-323-4204;
E-mail address: aa_ghoreyshi@nit.ac.ir (A.A. Ghoreyshi)

hydrogen discharge, and sensitivity of working lifetime to impurity of hydrogen are some drawbacks which restrict the application of metal hydrides [6,7]. Lack of advanced material as hydrogen storage media with easy handling system has made researchers seek for new storing systems such as microporous and nonstructural materials and/or their chemically modified types as physical or chemical adsorbents. One of these new materials is carbon nanotubes investigated as potential media for hydrogen storage due to their high surface area, light weight, and chemical stability [8].

Multi-walled nanotubes are preferred to single-walled ones for hydrogen storage due to numerous sites available on their outer surface, interior surface, and inter-planar spacing between the adjacent platelets [9]. However, a major weakness in structure of carbon nanotubes is their high aspect ratio which restricts their hydrogen storage capacity. Hydrogen adsorption and desorption is hindered due to the long path available for diffusion of hydrogen molecules into the interior surfaces of carbon nanotubes as well as the spatial restrictions for their movement [10]. Thus, it is essential to employ a technique to reduce the resistance for hydrogen entrance to the interior sites of carbon nanotubes. These techniques are based on the opening of carbon nanotubes edges and the creating of some defects on their outer surfaces [11]. Therefore, special activation processes are required to modify carbon nanotubes' surfaces in order to make a significant change in their specific surface area and porosity by removing the most reactive carbon atoms from their structure. It was found that basic solutions, such as NaOH and KOH, have the capability to be used as activating reagents due to their strong chemical etching effects [12-16].

Another approach for enhancement of hydrogen loading into the carbon nanotubes is coating a metal catalyst on their surface which converts molecular hydrogen to atomic hydrogen. This phenomenon is called hydrogen spillover. Hydrogen molecules after dissociation to atomic hydrogen diffuse through the support surface into the pores [17-19]. Based on the hydrogen spillover mechanism, atomic hydrogen is provided by the dissociation of molecular hydrogen on the catalytic sites available on the surface [20]. At the desorption step, atomic hydrogen diffuses back from the interior surface to outer surface of the support where it is converted to molecular form on the active catalytic sites, and then desorbs to the gas phase.

Although electroless deposition of Ni into CNT and development of CNT/Ni nanocomposites for H₂ storage have been investigated by some researchers [21,22], little has been done to enhance the H₂ storage capacity of the nanocomposite via surface activation of CNT, prior to metal deposition. To this end, the present study was carried out to find the

influence of activation of multi-walled carbon nanotube (MWCNT) by KOH on its hydrogen uptake performance. At the second step, nickel nanoparticles were deposited on the surface of activated MWCNTs using electroless deposition technique without pretreatment based on a simplified and cost-effective method. The effect of metal (Ni) loading on the hydrogen storage was also investigated. Additionally, adsorption equilibria and kinetics of H₂ adsorption on pristine, KOH activated and Ni coated MWCNT were analyzed based on the experimental data obtained in a volumetric adsorption apparatus.

2. Materials and methods

2.1. Materials

Multi-walled carbon nanotube (MWCNT), with inner diameter of 6-9 nm, synthesized via Catalytic Chemical Vapor Deposition (CCVD), was kindly provided by Professor A.R. Mohamed from School of Chemical Engineering, Universiti Sains Malaysia (USM) [23]. The purity of MWCNTs was above 95%; the remainder might include metallic catalysts, such as molybdenum and cobalt and amorphous carbon. The pristine sample, thereafter, is named as P-MWCNT. All chemicals used in activation and nickel deposition steps (supplied by Merck, Germany) were analytical grades and used without any further processing. High purity hydrogen gas (> 99.99%), supplied by Technical Gas Services Company, UAE, was used for H₂ sorption experiments.

2.2. Preparation of defective MWCNT by KOH

Defects were created on the surface of MWCNTs by KOH activation. The P-MWCNT was impregnated with KOH solution at a mass ratio of 4:1 (KOH: MWCNT) and placed in a shaker for effective mixing. The impregnated sample was dried at 383 K for 12 h. Then, the activation process was carried out in a horizontal furnace in which the sample was heated to activation temperature of 1073 K at a heating rate of 5 K/min under nitrogen flow of 300 ml/min for 1 h. After cooling the sample under N₂ to room temperature, the activated products were washed with 1 M HCl solution for 1 h to remove unreacted reagent. After doing the filtrating and washing processes several times with distilled water to neutrality, the sample was dried at 383 K overnight. The so-obtained MWCNT sample was named as A-MWCNT.

2.3. Nickel chemical deposition into the activated MWCNT

The activated MWCNT was doped with Ni nanoparticles using electroless deposition technique. Mallory and Hadju [24] employed electroless bath containing dimethylamine-borane (C₂H₁₀BN), and Haag et al. [25] used hydrazine (N₂H₄) as reducing agents. In both

Table 1. Composition of Ni electroless deposition bath.

Component	Quantity
MWCNT	0.2 (g)
Ni(NO ₃) ₂ .6H ₂ O 0.01 M	40 (ml)
Na ₂ .EDTA 0.1 M	1.5 (ml)
HCHO 37%	0.5 (ml)
Ethanol 99.99%	10 (ml)

of the mentioned research works, the treatment was aimed to modify the surface of the activated MWCNT substrate by plating a metallic precursor on it. In this work, surface activation pretreatment was not employed to initiate nickel deposition, as Ni(NO₃)₂ was used as the metal precursor. Composition of the alkaline deposition bath used in the present study is listed in Table 1. The alkaline deposition solution was composed of metal precursor, a reduction agent (HCHO), which was used for complete reduction of the metal precursor and ethanol that served as the carbon dispersion material. To start nickel chemical deposition, the activated MWCNT was first dispersed in ethanol solution, and the resultant suspension was stirred in Ni electroless deposition bath containing the metal precursor for 15 min at 318 K. Then, the mixture was filtered through a ceramic filter. The filtrate was washed several times with distilled water and dried at 383 K overnight. The Ni doped MWCNTs, thereafter, are referred to as Ni-MWCNT.

2.4. Characterization of MWCNTs samples

Textural properties of MWCNTs samples were studied through nitrogen adsorption/desorption isotherms which were measured by a surface area analyzer (QUANTACHROME, NOVA 2200) at the liquid nitrogen temperature (77 K). Prior to the adsorption measurements, all samples were degassed at 473 K for 6 h to remove moisture and other adsorbed contaminants. The specific surface area was calculated using the Brunauer-Emmett-Teller (BET) equation. The micropore and mesopore distributions were calculated by the Density Functional Theory (DFT) and Barrett-Joyner-Halenda (BJH) methods, respectively. Micropore volume (V_{mic}) was calculated from the adsorption isotherms by applying the Dubinin-Radushkevich (DR) equation. Total pore volume (V_t) was determined at $P/P_0 = 0.995$, and mesopore volume (V_{mes}) was calculated as the difference between V_t and V_{mic} . The amount of Ni deposited into MWCNTs was evaluated using an Inductively Coupled Plasma (ICP) spectrometer. Samples for ICP analysis were prepared by dissolving Ni-MWCNT in 3 M HNO₃ solution for 2 h to ensure that the Ni coating was completely dissolved in the acid solution. According to the measured Ni concentration in the solution, the percentage of Ni loading on MWCNT could be calculated. The struc-

tural changes in the MWCNT after KOH treatment were investigated by determining the orientation of the carbon structures through Raman spectroscopy performed using a spectrometer (Model SENTERRA) with an excitation power of 10 mW at wavelength of 785 nm. To investigate the morphological structure of the modified MWCNT samples and to confirm the Ni deposition into the MWCNT surface, SEM-EDS analysis was carried out on a Hitachi S-3400N Scanning Electron Microscope.

2.5. Hydrogen storage measurements

The hydrogen adsorption capacity of modified MWCNTs was measured at 288, 298, and 308 K in the pressure range of 0–45 bar using a volumetric method. A dual sorption cell apparatus was fabricated and used in this study for the assessment of hydrogen storage by MWCNTs. The schematic representation of the set-up is shown in Figure 1. The apparatus consisted of a central part formed by two high pressure cells interconnected by a valve named as reference cell (*R*) and pressure cell (*A*). The volumes of both reference and adsorption cells were 109 cm³. The total volume of the system, including the volume of the cells and connecting pipes, was determined by helium gas [26]. The gas pressure in both cells was measured by digital pressure gauges. The precision of the pressure transducer was 0.01 bar. The temperature of installation was controlled by a water bath. Prior to each experiment, MWCNTs were degassed at 473 K in an oven to remove any adsorbed contaminants. The sealing of the sample holder was carefully polished before every measurement. Before the measurement,

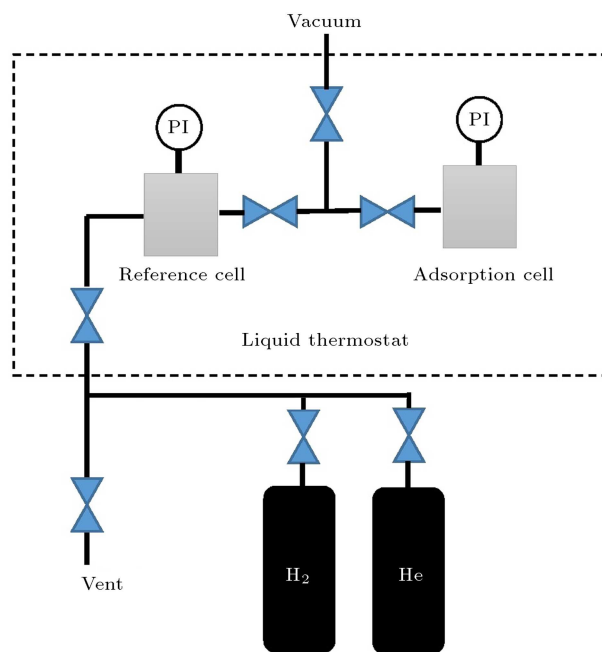


Figure 1. Schematic set-up of the volumetric apparatus used to measure hydrogen storage capacity.

the whole system was gradually evacuated for several hours to a pressure level below 0.1 mbar using a Rotary Vane vacuum pump (Edwards, U.K., Model E2M2). Then, the valves connecting the two high pressure cells were closed. At the beginning of each measurement, the reference cell was filled with high purity hydrogen gas. After 15 min, the whole system was considered to be in thermal equilibrium. Finally, the valve of the adsorption cell was opened, and when pressure equilibrium was obtained, valve was closed again. Due to the hydrogen adsorption, the adsorption cell pressure reduced until equilibrium conditions were obtained. The amount of adsorbed gas was calculated using the material balance, given by Eq. (1) and Peng-Rabinson equation of state, to determine hydrogen compressibility factor at equilibrium conditions:

$$\left[\frac{PV}{ZRT} \right]_{A_1} + \left[\frac{PV}{ZRT} \right]_{R_1} = \left[\frac{PV}{ZRT} \right]_{A_2} + \left[\frac{PV}{ZRT} \right]_{R_2} + n, \quad (1)$$

where P represents the pressure, T is the temperature, V denotes the volume, R is the universal gas constant, Z represents the gas compressibility factor (obtained from Soave-Redlich-Kwong (SRK) equation of state), and n is the adsorbed amount. Subscript 1 refers to the initial state, while subscript 2 represents the final equilibrium state. Subscripts R and A also refer to the reference and adsorption cells, respectively. Upon the attainment of n , Eq. (2) was used to calculate the hydrogen uptake capacity:

$$\text{Amount of stored hydrogen} = \frac{\left(\frac{n}{M} \right)}{TW} \times 100, \quad (2)$$

where M is the molecular weight of hydrogen, and TW is the sum of loaded MWCNTs and stored hydrogen weight during the hydrogen adsorption measurement.

3. Results and discussion

3.1. Characterization results

The Raman spectra of the pristine and chemically activated MWCNTs for a laser excitation wavelength of 785 nm are presented in Figure 2. Two important peaks observed around 1320 and 1587 cm^{-1} correspond to disordered (D-band) carbon lattice and graphitized (G-band) carbon lattice, respectively. The highly ordered and graphitic structure of P-MWCNT can be inferred from the sharp and intense G-band. After chemical activation, defects were created on the structure of MWCNT as deduced from the strong and sharp D-band appeared in the spectrum of A-MWCNT. In fact, the share of disordered carbon increased after activation of the MWCNT. The intensity ratio of D-band to G-band (ID/IG) gives some information about the level of defects created due to activation process.

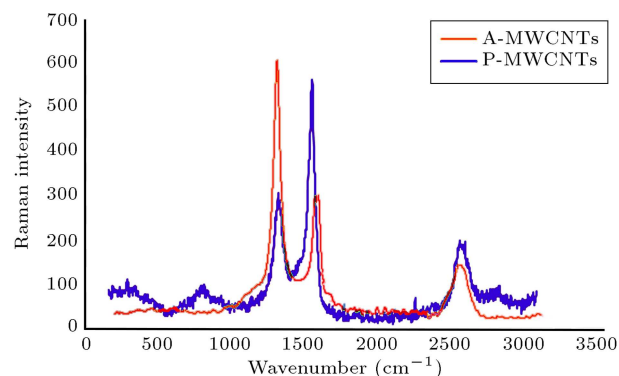


Figure 2. Raman spectra of pristine and chemically activated MWCNTs.

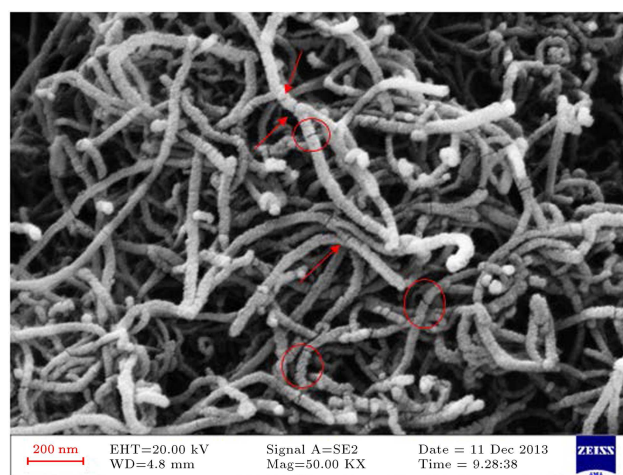


Figure 3. SEM image of the KOH activated MWCNTs.

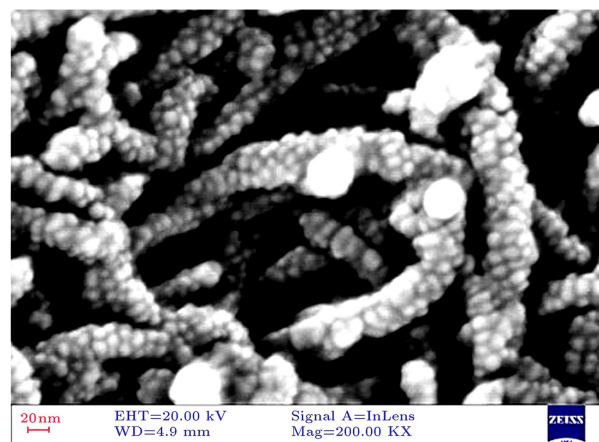
According to the Raman spectra, the calculated intensity ratios, (ID/IG), were 0.57 and 2.12 for P-MWCNT and A-MWCNT, respectively. This ratio was considerably higher for A-MWCNT, indicating that the carbon ring structure of P-MWCNT was successfully destroyed during KOH activation. Furthermore, the peak existing around 2700 cm^{-1} is assigned to G'-band, which is indicative of long-range order in a sample [27]. The intensity of this peak depends strongly on the metallicity of the nanotube [28]. As can be seen, the defect caused by the activation process influenced the electronic properties of MWCNTs sample.

Figure 3 illustrates the effect of KOH activation on the morphology of MWCNT. KOH activation created some defects on the structure of MWCNT as indicated by red circles and arrows in the image. The MWCNT, activated at KOH/MWCNT ratio of 4:1, roughly kept its tubular nanostructure morphology while the tubes were broken at some points and became shorter. The generated defects could increase the number of adsorption sites and facilitate the hydrogen transfer to the inner surfaces of MWCNT, and hence contribute to the enhancement of hydrogen uptake. The electroless deposition of metals into carbonaceous

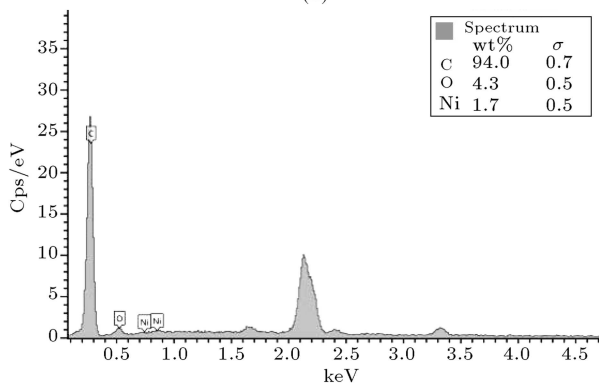
Table 2. Textural properties of the MWCNT samples.

Sample	S_{BET} (m^2/g)	V_{tot} (cm^3/g)	V_{mes} (cm^3/g)	V_{mic} (cm^3/g)	Microporosity fraction (%)
P-MWCNTs	340	0.41	0.277	0.133	32
A-MWCNTs	560	0.57	0.360	0.210	36

materials surfaces requires typically a pretreatment step recognized as sensitization and activation, prior to electroless deposition [18,24,29–32]. In this step, the substrate is immersed in SnCl_2 solution followed by immersion in PdCl_2 solution in which metallic Pd atoms act as seeds for the electroless deposition of the metal [23–25]. An alternative to bypass Sn-Pd pretreatment step is to deposit metal nanoparticles directly onto the activated MWCNT surface. This method also works because the surface of activated MWCNT includes numerous active sites in the form of hydroxyl groups (OH^-) which can serve as seeds for metal deposition. This approach was used in this study for Ni nanoparticle deposition into the activated MWCNT. The successful deposition of Ni into the activated MWCNT surface was confirmed by SEM-EDS analysis as illustrated in Figure 4. The amount



(a)



(b)

Figure 4. (a) SEM image of Ni doped MWCNT by the electroless deposition. (b) The corresponding EDS spectrum of Ni decorated MWCNT.

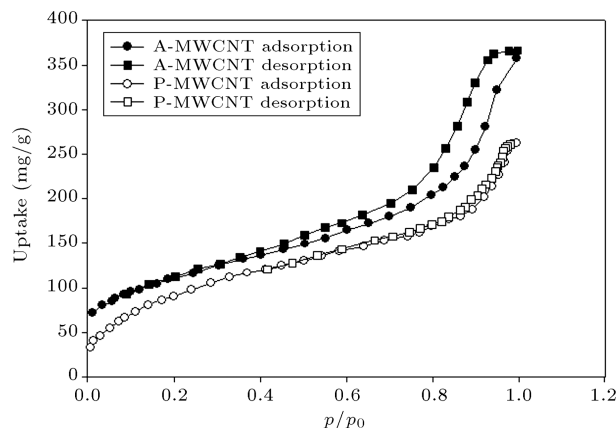


Figure 5. Adsorption-desorption isotherms for A-MWCNT and P-MWCNT.

of nickel deposited on the surface of A-MWCNT was determined by ICP spectroscopy which was 2.8 wt.% with respect to the Ni available in the electroless deposition bath.

The effect of KOH activation on porosity development of MWCNT was investigated by analyzing N_2 adsorption/desorption isotherms at 77 K for pristine and activated MWCNTs; the results are projected in Figure 5. As observed in the figure, the adsorption/desorption curve for KOH activated sample lies above the pristine one which indicates the higher potential of the activated sample for gas uptake. This was confidently attributed to the improvement made in the textural properties of the activated sample as also evidenced by the results summarized in Table 2.

The textural properties of both pristine and KOH activated MWCNTs are listed in Table 2. As the results show, the chemical activation is effective in enhancing the BET surface area and micropore and mesopore volumes of the MWCNT. Heat treatment of MWCNT with KOH removes carbon atoms in the form of carbon monoxide or carbon dioxide which leads to the porosity development of the P-MWCNT as well as creation of some defects on its graphitic structure [33,34]. The chemical activation also improved the microporosity fraction ($V_{\text{mic}}/V_{\text{tot}}$) of the sample which is expected to play a significant role in facilitating hydrogen adsorption into MWCNT.

3.2. Hydrogen storage results

The hydrogen storage capacity of MWCNT samples was tested at different temperatures at fixed pressure of 45 bar; the results of this investigation are pre-

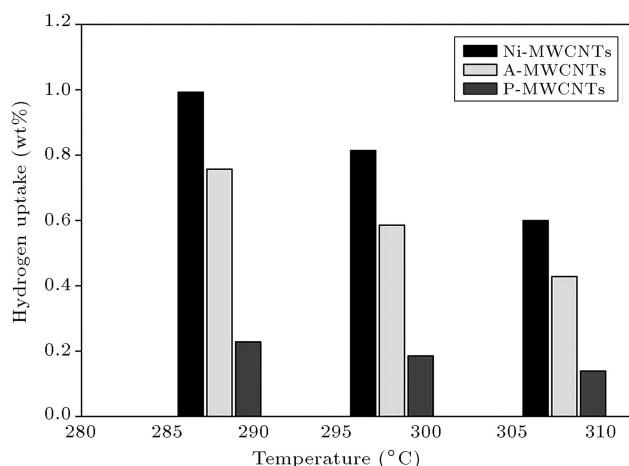


Figure 6. Hydrogen uptake of MWCNT samples at different temperatures at 45 bar.

sented in Figure 6. The hydrogen storage capacity decreased as the temperature increased. The hydrogen storage capacity of A-MWCNT sample was remarkably higher than the pristine sample owing to the improved porosity. Indeed, development of specific surface area and pore volume in A-MWCNT, resulted from defects generated on the external surface during activation process, made a great contribution to the enhancement of hydrogen storage capacity. However, the hydrogen storage ability of chemically activated sample was further enhanced after nickel deposition. The highest hydrogen sorption capacity of ~ 1 wt% was obtained with nickel doped MWCNT (Ni-MWCNT) sample at 288 K under pressure of 45 bar. The enhancement in hydrogen storage capacity of MWCNT after Ni deposition could be attributed to the spillover mechanism in which hydrogen molecules are transformed on the Ni decorated surfaces of MWCNT [31].

The results of the current work were compared to those of other reports available in the literature, as summarized in Table 3. A comparison of the results reveals that our developed nanocomposite has a reasonable H_2 sorption performance.

3.3. Determination of adsorption isotherm

Adsorption isotherm models provide qualitative information on the nature of adsorbate-adsorbent interaction. They also give some insight into how gas molecules accumulate on the adsorbent surface or in porous media and how the accumulation of gas varies with pressure at constant temperature [26].

Langmuir model is one of the well-known isotherm models that assumes a monolayer coverage of adsorbate on the homogeneous surface with no interaction between the adsorbate molecules on the adjacent sites [42]. The nonlinear form of Langmuir isotherm model can be expressed by the following equation:

$$W_e = \frac{W_m K_L P}{1 + K_L P}, \quad (3)$$

where W_e is the amount of H_2 adsorbed per unit mass of MWCNT (mg/g); W_m is the maximum amount of H_2 adsorbed (mg/g), and K_L (bar^{-1}) is the Langmuir adsorption constant which is related to the energy of adsorption.

In contrast to the Langmuir model, Freundlich isotherm model considers a multi-layer adsorption coverage on the heterogeneous active sites with different energies. This equation is given as follows:

$$W_e = K_F P^{1/n}, \quad (4)$$

where K_F is the Freundlich adsorption constant ($1/\text{bar}^{1/n}$), and n represents bond energies between hydrogen molecules and the adsorbent.

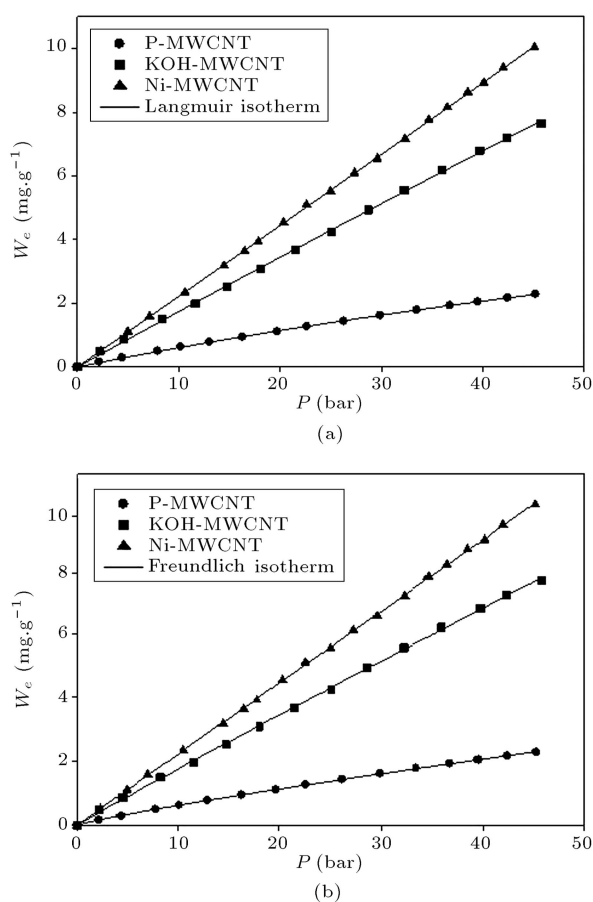
The Langmuir and Freundlich isotherm models were used to interpret the experimental data. Figures 7(a) and 7(b) illustrate the best fit to the equilibrium data for Langmuir and Freundlich isotherms, respectively, at 288 K for P-MWCNT, A-MWCNT, and Ni-MWCNTs samples. The isotherm parameters were obtained from non-linear fit of equilibrium data to the isotherm models. The values of Langmuir and Freundlich constants for each sample at 288, 298, and 308 K are listed in Table 4.

Table 3. Comparison of the results of the current work to those reported in the literature for hydrogen storage.

Material	Hydrogen uptake (wt%)	Temperature (K)	Pressure (bar)	Reference
Heat-treated MWCNT	0.4	298	5	[35]
Activated-MWCNT	0.54	77	1	[36]
Pd-MWCNT	0.8	123	45	[37]
MWCNT-TiO ₂	0.9	373	N/A	[38]
SWCNT/Pt-C	0.25	298	45	[39]
K-SiCNT	0.4	298	100	[40]
Pt/Pd activated carbon	0.6	298	45	[41]
This work	1	288	45	—

Table 4. Langmuir and Freundlich isotherm constants for adsorption of H₂ onto P-MWCNT, A-MWCNT, and Ni-MWCNT.

Isotherm	Parameters								
	Ni-MWCNT			A-MWCNT			P-MWCNT		
Langmuir	288 K	298 K	308 K	288 K	298 K	308 K	288 K	298 K	308 K
W_m (mg.g ⁻¹)	1105	595.33	659.5	218.65	42.27	40.34	10.81	9.75	5.79
K_L (bar ⁻¹)	0.0002	0.0003	0.0002	0.0008	0.0036	0.0026	0.0059	0.0052	0.0068
R^2	0.9999	0.9998	0.9998	0.9995	0.9998	0.9998	0.9999	0.9998	0.9998
Freundlich									
K_F (bar ^{-1/n})	0.2178	0.1752	0.1302	0.1838	0.1821	0.1196	0.0834	0.0636	0.0530
n	0.993	0.991	0.993	1.022	1.093	1.065	1.148	1.126	1.169
R^2	0.9999	0.9998	0.9998	0.9995	0.9998	0.9998	0.9999	0.9996	0.9995

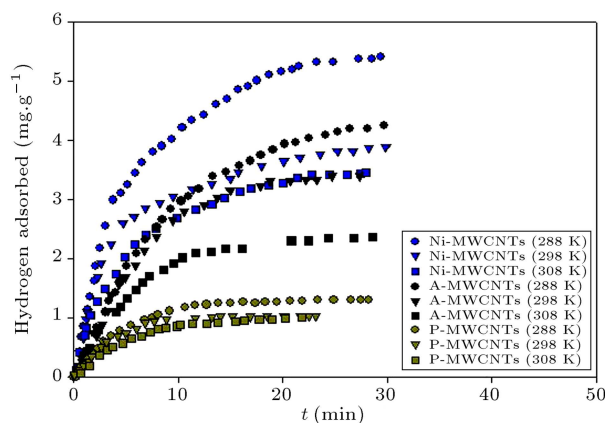
**Figure 7.** (a) Langmuir and (b) Freundlich isotherm models for adsorption of H₂ into P-MWCNT, A-MWCNT, and Ni-MWCNT at 288 K.

As can be seen in Table 4, both isotherm models fitted the equilibrium data with very high correlation coefficients ($R^2 > 0.999$). One of the main characteristics of Langmuir adsorption constant (K_L) is its decrease with increase of temperature [26]; however, in this experiment, this constant fluctuates with increase in temperature, showing that this model is not reliable for interpretation of hydrogen adsorption data. On the contrary, Freundlich constant (K_F) reduced with increase in temperature, suggesting that the hydrogen

adsorption is favorable at low temperature. Furthermore, since activated carbons are energetically heterogeneous, it is reasonable to conclude that Freundlich isotherm model is a suitable one for explanation of adsorption on MWCNT samples.

3.4. Adsorption kinetics studies

The mass uptake of hydrogen as a function of time at 288, 298, and 308 K and 25 bar is shown in Figure 8 for P-MWCNT, A-MWCNT, and Ni-MWCNT samples. The adsorption curves for all samples show an initial rapid increase followed by a period of much slower increase, approaching an equilibrium at the late stage. At the initial period of adsorption, hydrogen molecules are subjected to a plenty of free adsorption sites on the adsorbent surface which can be easily adsorbed on them. The rate of adsorption becomes slow as monolayer coverage is completed. From Figure 8, it is clear that the initial hydrogen uptake by both the activated and Ni doped MWCNT samples has substantially improved as compared to the pristine sample. The enhanced textural properties and catalytic effect are accounted for superior adsorption kinetics of A-MWCNT and Ni-MWCNT compared to that of P-MWCNT. Zaluski et al. [43] reported the catalytic role of transition metal alloys on the enhancement of hydrogen storage.

**Figure 8.** Hydrogen adsorption kinetic data for the MWCNT samples at 25 bar.

Likewise, Lupu et al. [44] reported enhanced hydrogen uptake by Pd doped carbon nanofibers. The spillover of hydrogen on metal oxide coated MWNT was also reported by Lueking and Yang [19,45]. Similar results were also found by Lin et al. [30] who worked on Ni doped CNT.

Study of adsorption kinetics gives an insight into how fast the adsorption on an adsorbent surface takes place. In addition, modeling of kinetic data based on the amount of uptake as a function of time can be used to recognize the rate-determining step in adsorption process. These models generally fall into two categories. In the first classification called “reaction” models, the entire adsorption process is included in a single step [46]; the second group includes “diffusion” models in which the individual resistances available for mass transport from gas bulk to adsorbent pores are modelled as sequential steps. Two well-known kinetic models with frequent applications in gas adsorption are pseudo-first-order [47] and pseudo-second-order [48] models which are classified as reaction models. They have been extensively applied for describing the gas uptake kinetics. The pseudo-first-order model can be expressed as follows:

$$\frac{dW_t}{dt} = K_1(W_e - W_t), \quad (5)$$

where W_e is the amount of hydrogen adsorbed at equilibrium (mg/g), W_t is the amount of hydrogen adsorbed at time t (mg/g), and K_1 is the equilibrium rate constant of pseudo-first-order equation (1/min). Integrating Eq. (3) with respect to the initial condition at $t = t_0$ and $W_t = 0$ gives:

$$\ln\left(1 - \frac{W_t}{W_e}\right) = -K_1 t. \quad (6)$$

Plotting $\ln(1 - \frac{W_t}{W_e})$ versus t ($t > t_0$) is linear if pseudo-first-order model is applicable, and K_1 can be determined from the slope of the plot.

The pseudo second-order equation is expressed as follows:

$$\frac{dW_t}{dt} = K_2(W_e - W_t)^2, \quad (7)$$

where K_2 is the equilibrium rate constant (g/mg.min). Applying the initial condition (at $t = t_0$ and $W_t = 0$) in the integrated form of above equation and rearranging

it gives the following equation:

$$\frac{t - t_0}{W_t} = \frac{1}{K_2 W_e^2} + \frac{t - t_0}{W_e}. \quad (8)$$

The plot of $\frac{t-t_0}{W_t}$ versus t ($t > t_0$) gives a straight line with slope of $\frac{1}{W_e}$ if the system follows the pseudo second-order equation.

The kinetic data obtained for P-MWCNT, A-MWCNT, and Ni-MWCNT samples at 288 K and initial pressure of 25 bar (see Figure 8) were plotted in a linear form based on Eqs. (6) and (8) as exhibited in Figure 9(a) and (b), respectively. All kinetic data corresponding to all three samples were well fitted to the pseudo-second-order equation. The constants and parameters of this model determined from linear fit (Figure 9(b)) are presented in Table 5.

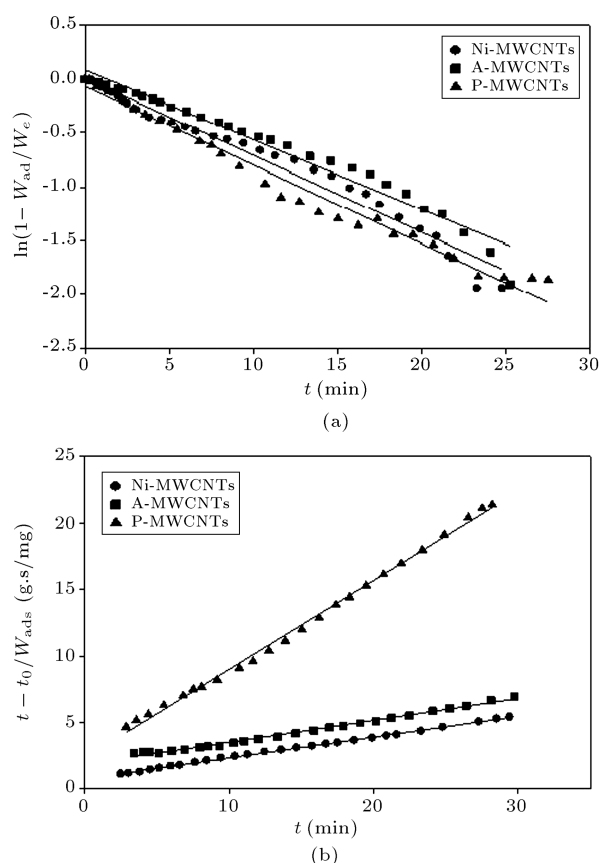


Figure 9. (a) Pseudo-first-order and (b) pseudo-second-order model fits of the kinetic data for H_2 adsorption onto MWCNT samples at 288 K and 25 bar.

Table 5. Pseudo-second-order rate constants and parameters obtained for H_2 adsorption into different MWCNT samples at 288, 298, and 308 K and 25 bar.

Temperature (K)	P-MWCNT			A-MWCNT			Ni-MWCNT		
	W_e	K_2	R^2	W_e	K_2	R^2	W_e	K_2	R^2
288	1.490	0.192	0.996	6.157	0.0137	0.995	6.40	0.0315	0.998
298	1.167	0.346	0.994	4.370	0.0331	0.992	5.10	0.0526	0.998
308	1.265	0.152	0.994	2.890	0.0632	0.993	4.13	0.0473	0.999

4. Conclusion

In this study, it was attempted to enhance the hydrogen storage capacity of MWCNT through some surface modifications. At the first step, the hydrogen uptake capacity of MWCNT was enhanced using chemical activation by KOH. The structural defects generated during activation of MWCNT improved its textural properties in terms of surface area, total and micropore volumes as well as microporosity fraction which resulted in its enhanced hydrogen uptake. At the second step, electroless deposition technique was applied for preparation of Ni-MWCNT composite. The Ni introduced into the MWCNT skeleton played a significant role in the enhancement of hydrogen storage capacity through the catalytic effect via the spillover mechanism. In addition to higher adsorption capacity, Ni doped MWCNT demonstrated faster adsorption kinetics compared to pristine sample. The maximum storage capacity achieved by Ni doped MWCNT was ~ 1 wt.% at 288 K and 45 bar. Finally, kinetics of hydrogen adsorption by pristine and modified samples of MWCNTs was analyzed using pseudo-first-order and pseudo-second-order kinetic models. From the modeling results, it was found that the kinetic data for H₂ adsorption could be suitably described by the pseudo-second-order model.

References

- Singh, P., Kulkarni, M.V., Gokhale, S.P., Chikkali, S.H. and Kulkarni, C.V. "Enhancing the hydrogen storage capacity of Pd-functionalized multi-walled carbon nanotubes", *Appl. Surf. Sci.*, **258**(8), pp. 3405-3409 (2012).
- Martis, P., Venugopal, B., Delhalle, J. and Mekhalif, Z. "Selective decoration of nickel and nickel oxide nanocrystals on multiwalled carbon nanotubes", *J. Solid State Chem.*, **184**(5), pp. 1245-1250 (2011).
- Ma, L., Zhang, J.-M. and Xu, K.-W. "Hydrogen storage on nitrogen induced defects in palladium-decorated graphene: A first-principles study", *Appl. Surf. Sci.*, **292**(0), pp. 921-927 (2014).
- Im, J.S., Yun, J., Kang, S.C., Lee, S.K. and Lee, Y.-S. "Hydrogen adsorption on activated carbon nanotubes with an atomic-sized vanadium catalyst investigated by electrical resistance measurements", *Appl. Surf. Sci.*, **258**(7), pp. 2749-2756 (2012).
- Yürüm, Y., Taralp, A. and Veziroglu, T.N. "Storage of hydrogen in nanostructured carbon materials", *Int. J. Hydrogen Energy*, **34**(9), pp. 3784-3798 (2009).
- Grochala, W. and Edwards, P.P. "Thermal decomposition of the non-interstitial hydrides for the storage and production of hydrogen", *Chem. Rev.*, **104**(3), pp. 1283-1316 (2004).
- Bogdanović, B. and Schwickardi, M. "Ti-doped alkali metal aluminium hydrides as potential novel reversible hydrogen storage materials", *J. Alloys Compd.*, **253**, pp. 1-9 (1997).
- Morel, M., Mosquera, E., Diaz-Droguett, D.E., Carvajal, N., Roble, M., Rojas, V. and Espinoza-González, R. "Mineral magnetite as precursor in the synthesis of multi-walled carbon nanotubes and their capabilities of hydrogen adsorption", *Int. J. Hydrogen Energy*, **40**(45), pp. 15540-15548 (2015).
- Wang, Y., Wu, J. and Wei, F. "A treatment method to give separated multi-walled carbon nanotubes with high purity, high crystallization and a large aspect ratio", *Carbon*, **41**(15), pp. 2939-2948 (2003).
- Chen, C.-H. and Huang, C.-C. "Enhancement of hydrogen spillover onto carbon nanotubes with defect feature", *Microporous Mesoporous Mater.*, **109**(1), pp. 549-559 (2008).
- Mosquera, E., Diaz-Droguett, D.E., Carvajal, N., Roble, M., Morel, M. and Espinoza, R. "Characterization and hydrogen storage in multi-walled carbon nanotubes grown by aerosol-assisted CVD method", *Diamond Relat. Mater.*, **43**, pp. 66-71 (2014).
- Raymundo-Pinero, E., Azais, P., Cacciaguerra, T., Cazorla-Amorós, D., Linares-Solano, A. and Béguin, F. "KOH and NaOH activation mechanisms of multiwalled carbon nanotubes with different structural organisation", *Carbon*, **43**(4), pp. 786-795 (2005).
- Chen, C.-H. and Huang, C.-C. "Hydrogen storage by KOH-modified multi-walled carbon nanotubes", *Int. J. Hydrogen Energy*, **32**(2), pp. 237-246 (2007).
- Jordá-Beneyto, M., Suárez-García, F., Lozano-Castelló, D., Cazorla-Amorós, D. and Linares-Solano, A. "Hydrogen storage on chemically activated carbons and carbon nanomaterials at high pressures", *Carbon*, **45**(2), pp. 293-303 (2007).
- Wu, F.-C., Tseng, R.-L. and Juang, R.-S. "Comparisons of porous and adsorption properties of carbons activated by steam and KOH", *J. Colloid Interface Sci.*, **283**(1), pp. 49-56 (2005).
- Jiménez, V., Díaz, J.A., Sánchez, P., Valverde, J.L. and Romero, A. "Influence of the activation conditions on the porosity development of herringbone carbon nanofibers", *Chem. Eng. J.*, **155**(3), pp. 931-940 (2009).
- Bhowmick, R., Rajasekaran, S., Friebel, D., Beasley, C., Jiao, L., Ogasawara, H., Dai, H., Clemens, B. and Nilsson, A. "Hydrogen spillover in pt-single-walled carbon nanotube composites: formation of stable C-H bonds", *J. Am. Chem. Soc.*, **133**(14), pp. 5580-5586 (2011).
- Wang, Y., Wang, K., Guan, C., He, Z., Lu, Z., Chen, T., Liu, J., Tan, X., Yang Tan, T.T. and Li, C.M. "Surface functionalization-enhanced spillover effect on hydrogen storage of Ni-B nanoalloy-doped activated carbon", *Int. J. Hydrogen Energy*, **36**(21), pp. 13663-13668 (2011).

19. Lueking, A. and Yang, R.T. "Hydrogen spillover from a metal oxide catalyst onto carbon nanotubes - implications for hydrogen storage", *J. Catal.*, **206**(1), pp. 165-168 (2002).
20. Lachawiec, A.J., Qi, G. and Yang, R.T. "Hydrogen storage in nanostructured carbons by spillover: bridge-building enhancement", *Langmuir*, **21**(24), pp. 11418-11424 (2005).
21. Rahimi, N., Doroodmand, M.M., Sabbaghi, S. and Sheikhi, M.H. "Electrochemical hydrogen evolution of multi-walled carbon nanotube/micro-hybrid composite decorated with Ni nanoparticles as catalyst through electroless deposition process", *Mater. Sci. Eng., C*, **33**(6), pp. 3173-3179 (2013).
22. Lin, K.-Y., Tsai, W.-T. and Chang, J.-K. "Decorating carbon nanotubes with Ni particles using an electroless deposition technique for hydrogen storage applications", *Int. J. Hydrogen Energy*, **35**(14), pp. 7555-7562 (2010).
23. Yeoh, W.-M., Lee, K.-Y., Chai, S.-P., Lee, K.-T. and Mohamed, A.R. "Synthesis of high purity multi-walled carbon nanotubes over Co-Mo/MgO catalyst by the catalytic chemical vapor deposition of methane", *New Carbon Mater.*, **24**(2), pp. 119-123 (2009).
24. Mallory, G.O. and Hajdu, J.B., *Electroless Plating: Fundamentals and Applications*, William Andrew (1990).
25. Haag, S., Burgard, M. and Ernst, B. "Pure nickel coating on a mesoporous alumina membrane: Preparation by electroless plating and characterization", *Surf. Coat. Technol.*, **201**(6), pp. 2166-2173 (2006).
26. Khalili, S., Ghoreyshi, A.A., Jahanshahi, M. and Pirzadeh, K. "Enhancement of carbon dioxide capture by amine-functionalized multi-walled carbon nanotube", *CLEAN-Soil, Air, Water*, **41**(10), pp. 939-948 (2013).
27. Jorio, A., Pimenta, M., Souza Filho, A., Saito, R., Dresselhaus, G. and Dresselhaus, M. "Characterizing carbon nanotube samples with resonance Raman scattering", *New J. Phys.*, **5**(1), p. 139 (2003).
28. Kim, K.K., Park, J.S., Kim, S.J., Geng, H.Z., An, K.H., Yang, C.-M., Sato, K., Saito, R. and Lee, Y.H. "Dependence of Raman spectra G' band intensity on metallicity of single-wall carbon nanotubes", *Phys. Rev. B: Condens. Matter*, **76**(20), p. 205426 (2007).
29. Chen, C.-Y., Lin, K.-Y., Tsai, W.-T., Chang, J.-K. and Tseng, C.-M. "Electroless deposition of Ni nanoparticles on carbon nanotubes with the aid of supercritical CO₂ fluid and a synergistic hydrogen storage property of the composite", *Int. J. Hydrogen Energy*, **35**(11), pp. 5490-5497 (2010).
30. Lin, K.-Y., Tsai, W.-T. and Yang, T.-J. "Effect of Ni nanoparticle distribution on hydrogen uptake in carbon nanotubes", *J. Power Sources*, **196**(7), pp. 3389-3394 (2011).
31. Kim, B.-J., Lee, Y.-S. and Park, S.-J. "A study on the hydrogen storage capacity of Ni-plated porous carbon nanofibers", *Int. J. Hydrogen Energy*, **33**(15), pp. 4112-4115 (2008).
32. Wu, Z., Ge, S., Zhang, M., Li, W. and Tao, K. "Synthesis of nickel nanoparticles supported on metal oxides using electroless plating: Controlling the dispersion and size of nickel nanoparticles", *J. Colloid Interface Sci.*, **330**(2), pp. 359-366 (2009).
33. Niu, J.J. and Wang, J.N. "Effect of temperature on chemical activation of carbon nanotubes", *Solid State Sciences*, **10**(9), pp. 1189-1193 (2008).
34. Meng, L.-Y. and Park, S.-J. "Effect of heat treatment on CO₂ adsorption of KOH-activated graphite nanofibers", *J. Colloid Interface Sci.*, **352**(2), pp. 498-503 (2010).
35. Geng, H.-Z., Kim, T.H., Lim, S.C., Jeong, H.-K., Jin, M.H., Jo, Y.W. and Lee, Y.H. "Hydrogen storage in microwave-treated multi-walled carbon nanotubes", *Int. J. Hydrogen Energy*, **35**(5), pp. 2073-2082 (2010).
36. Lee, S.-Y. and Park, S.-J. "Influence of the pore size in multi-walled carbon nanotubes on the hydrogen storage behaviors", *J. Solid State Chem.*, **194**, pp. 307-312 (2012).
37. Banerjee, S., Dasgupta, K., Kumar, A., Ruz, P., Vishwanadh, B., Joshi, J. and Sudarsan, V. "Comparative evaluation of hydrogen storage behavior of Pd doped carbon nanotubes prepared by wet impregnation and polyol methods", *Int. J. Hydrogen Energy*, **40**(8), pp. 3268-3276 (2015).
38. Silambarasan, D., Kanmani, M., Iyakutti, K., Jeyanthinath, M., Ravindran, T.R. and Vasu, V. "Investigation of hydrogen storage in MWCNT-TiO₂ composite", *Physica E*, **80**, pp. 207-211 (2016).
39. Yang, F.H., Lachawiec, A.J. and Yang, R.T. "Adsorption of spillover hydrogen atoms on single-wall carbon nanotubes", *J. Phys. Chem. B*, **110**(12), pp. 6236-6244 (2006).
40. Barghi, S.H., Tsotsis, T.T. and Sahimi, M. "Experimental investigation of hydrogen adsorption in doped silicon-carbide nanotubes", *Int. J. Hydrogen Energy*, **41**(1), pp. 369-374 (2016).
41. Geng, Z., Wang, D., Zhang, C., Zhou, X., Xin, H., Liu, X. and Cai, M. "Spillover enhanced hydrogen uptake of Pt/Pd doped corncob-derived activated carbon with ultra-high surface area at high pressure", *Int. J. Hydrogen Energy*, **39**(25), pp. 13643-13649 (2014).
42. Pirzadeh, K. and Ghoreyshi, A.A. "Phenol removal from aqueous phase by adsorption on activated carbon prepared from paper mill sludge", *Desalin. Water Treat.*, **52**(34-36), pp. 6505-6518 (2014).
43. Zaluski, L., Zaluska, A., Tessier, P., Ström-Olsen, J.O. and Schulz, R. "Catalytic effect of Pd on hydrogen absorption in mechanically alloyed Mg₂Ni, LaNi₅ and FeTi", *J. Alloys Compd.*, **217**(2), pp. 295-300 (1995).
44. Lupu, D., Radu Biriş, A., Mişan, I., Jianu, A., Holzhüter, G. and Burkel, E. "Hydrogen uptake by carbon nanofibers catalyzed by palladium", *Int. J. Hydrogen Energy*, **29**(1), pp. 97-102 (2004).

45. Lueking, A. and Yang, R.T. "Hydrogen storage in carbon nanotubes: residual metal content and pretreatment temperature", *AIChE Journal*, **49**(6), pp. 1556-1568 (2003).
46. Ruthven, D.M., *Principles of Adsorption and Adsorption Processes*, John Wiley & Sons (1984).
47. Lagergren, S. "About the theory of so-called adsorption of soluble substances", *Kungliga Svenska Vetenskapsakademiens Handlingar*, **24**(4), pp. 1-39 (1898).
48. Ho, Y.-S. and McKay, G. "Pseudo-second order model for sorption processes", *Process Biochem.*, **34**(5), pp. 451-465 (1999).

Biographies

Adel Hoseini obtained his BSc from Chemical Engineering Department of Mazandaran University in 2010. He continued his education in Babol Noshirvani University of Technology and received his MSc in Chemical Engineering, in 2013. He carried out his thesis under the supervision of Professor Ali Asghar Ghoreyshi entitled "Enhancement of hydrogen storage on multi-walled carbon nanotube through KOH activation and nickel nanoparticle deposition".

Ali Asghar Ghoreyshi obtained his BSc from Chemical Engineering Department of Sharif University of Technology, Tehran, Iran, in 1985. His studies continued in Sharif University of Technology for MSc degree which ended in 1989 doing a thesis entitled "Deaeration of industrial water in packed tower, modelling and simulation". He received his PhD from University of Surrey, Guildford, UK, in 2001, in membrane separation after doing his thesis entitled "Multicomponent transport across nonporous homogeneous membranes". Dr. Ghoreyshi is serving as a Professor in Babol

Noshirvani University of Technology with 24 years of teaching experience. Currently, he is the dean of research and technology in this university.

He has published more than 100 articles in international journals. He has also published three books in adsorption and fuel cell areas. His research interests include membrane separation, fuel cell technology, modeling and simulation of separation processes, adsorption (gases and liquids), and water and wastewater treatment.

Kasra Pirzadeh is a PhD student of Chemical Engineering in Babol Noshirvani University of Technology. He is working on electrochemical synthesis of metal organic frameworks for CO₂/CH₄ storage and separation under the supervision of Professor Ali Asghar Ghoreyshi. He obtained his MSc degree in 2012 from Babol Noshirvani University of Technology. He worked on phenol adsorption from aqueous solution on sewage sludge based activated carbon. He received his BSc from Mazandaran University in 2010. He is the co-author of several publications supervised by Professor Ali Asghar Ghoreyshi.

Maedeh Mohammadi is an Assistant Professor in Faculty of Chemical Engineering at Babol Noshirvani University of Technology. She is currently the co-leader of the biotechnology and bioenergy research lab of BUT, focusing on several research projects in this area. She received her BSc degree from Isfahan University of Technology, in 2004, MSc and PhD degrees (with hon.) from University of Mazandaran in 2007 and 2012, all in Chemical Engineering. Dr. Mohammadi's research interests are focused on bioenergy and biofuel production, renewable energy, carbon dioxide conversion and utilization, and adsorption processes.